

Author: Kyriaki Metheniti, HNMS
Showcase Title: A case of Rapid Cyclogenesis
Time frame: February 6 to February 7, 2012
Study region: Eastern Mediterranean, Ionian Sea

A case of Rapid Cyclogenesis over Ionian Sea on February 6th, 2012

Introduction

A surface depression originated at the Gulf of Sidra across the Libyan coast of northern Africa on February 6th, 2012 deepens rapidly as it moves northwards atop Ionian Sea, producing deep convection with excessive rainfall amounts over Greece and a very strong surface pressure gradient, with surface wind speeds exceeding 41 kts (9 beaufort) for many ground based stations. Cancellation of all activities in the marine environment, flooding and vegetation and structural damage over most parts of the country result from this particular low pressure system and its eastward movement. The intensity of both the wind field and the convective precipitation for this event is quite well forecasted and on-time warnings for Port Authorities and the public are issued and broadcasted.

General meteorological context

The pre-existing (before 06-02-2012) weather pattern is characterized by high pressures dominating from Russia to the Azores and cold air that has overspread large portions of central Europe and Asia (temperatures ranging from -10 to -24° C at 850 hPa (fig.2)). There is an intense longwave trough centered over the northern coast of Algeria and the Tyrrhenian Sea, developing between two jet streaks present in the upper troposphere (fig.1), a main polar jet stream extending from N. Atlantic through the United Kingdom up to Spain and the subtropical jet stream extending from Algeria to Turkey. This highly meridional flow pattern persists over Europe (fig.3), with the primary change being a rapidly evolving cyclone over central Mediterranean Sea (fig.4), which develops from the aforementioned longwave mid-level trough and is enhanced by stratospheric air extruding well within the troposphere (fig.4). Figures 5 and 6 depict an 18 hPa drop in mean sea level pressure in just 12 hours.

Regarding this developing surface depression, the main forecast challenges are its trajectory and minimum pressure, with model outputs (from ECMWF and GFS) converging to a depression with pressure dropping below 995 hPa at the Ionian Sea, before filling over land (observed minimum pressure 982 hPa (fig.6) centered over central Ionian Sea). The strong pressure gradients surrounding this feature are expected to produce surface wind speeds reaching strong gale forces.

Convection is reasonably anticipated under the unstable configuration of warm air being advected beneath the colder mid-levels (fig.2) by the persistent southerly flow associated with the low pressure system that moves slowly to the north. Abundant moisture advection that is also expected, is pointing towards Greece and the warm plume of air advected northward over maritime areas into land, will lead to continuous convective rainfall over western Greece, with high probability of being severe. Following the ageostrophic deflection of the low level wind in response to the deepening of the depression, directional shear increases with time within an unstable warm, allowing organized multicells to evolve with strong wind gusts and heavy rainfall (Tuschy, from the Estofex.org experiment). The strong temperature gradient (fig.2) marks the position of the surface frontal zone. As its warm sector shifts while the depression is moving to the east, strong wind gusts and heavy rainfall are expected to expand eastwards.

A strong gale warning was issued and broadcasted in advance, that was well forecasted since surface winds speeds reached 59kts over the maritime areas. A warning for excessive convective precipitation was issued and broadcasted as well. Excessive rainfall did actually occur, with rain rates of 118mm being recorded over the southwestern part of the country.

* Plots in figures 1 - 3 and 5 - 6 are computed using the ERA-Interim reanalysis of ECMWF model

** Images in fig.4, 8a, 8b and 9a, 9b are from the eport archive of eumetrain.org

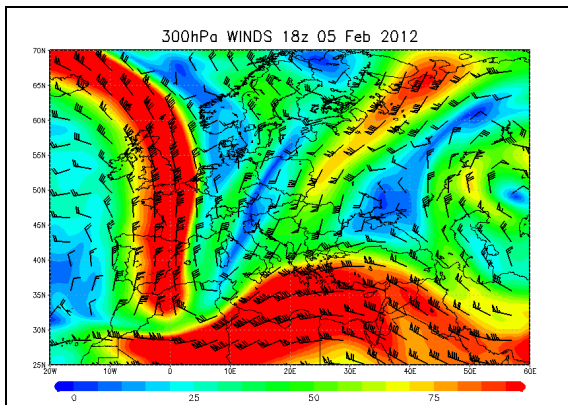


Fig.1: Winds at 300hPa, 05-02-2012/18 utc

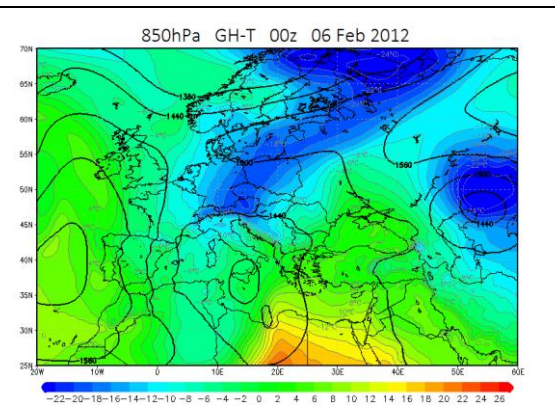


Fig.2: Geopotential height/temperature at 850hPa, 06-02-2012/00 utc

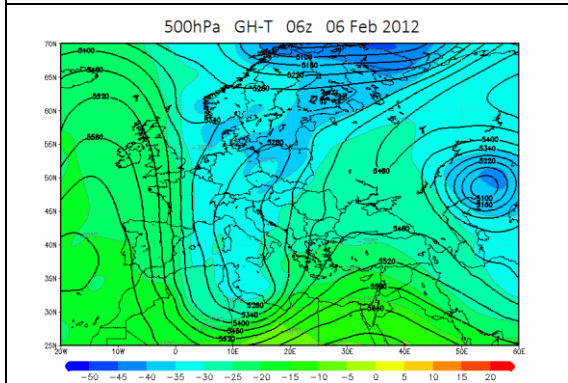


Fig.3: Geopotential height/temperature at 500hPa, 06-02-2012/06 utc

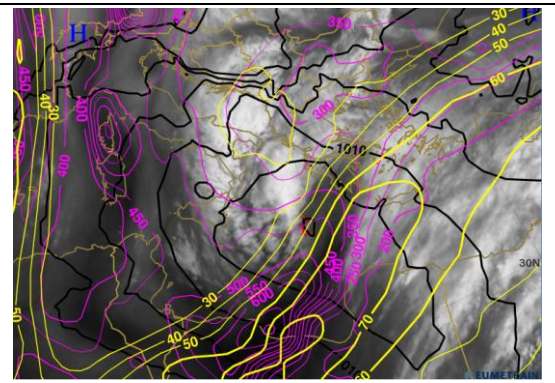


Fig.4: Height in hPa where IPV=1.5PVU / mslp by 5hPa / isotachs at 300hPa, 06-02-2012/06 utc

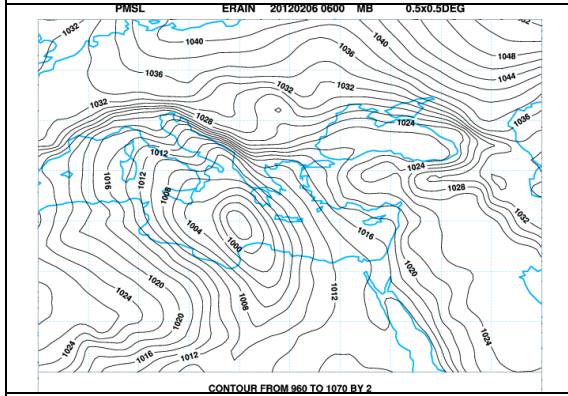


Fig.5: Mean sea level pressure contours by 2 hPa, 06-02-2012/06 utc

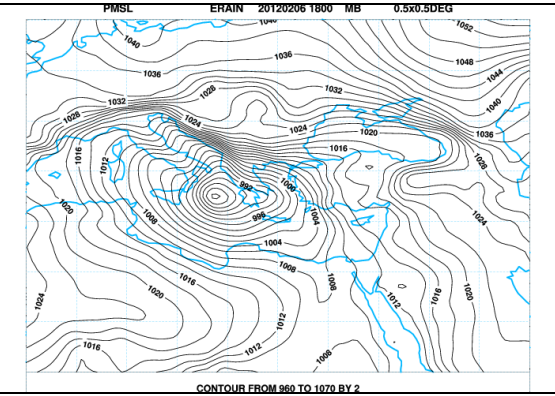
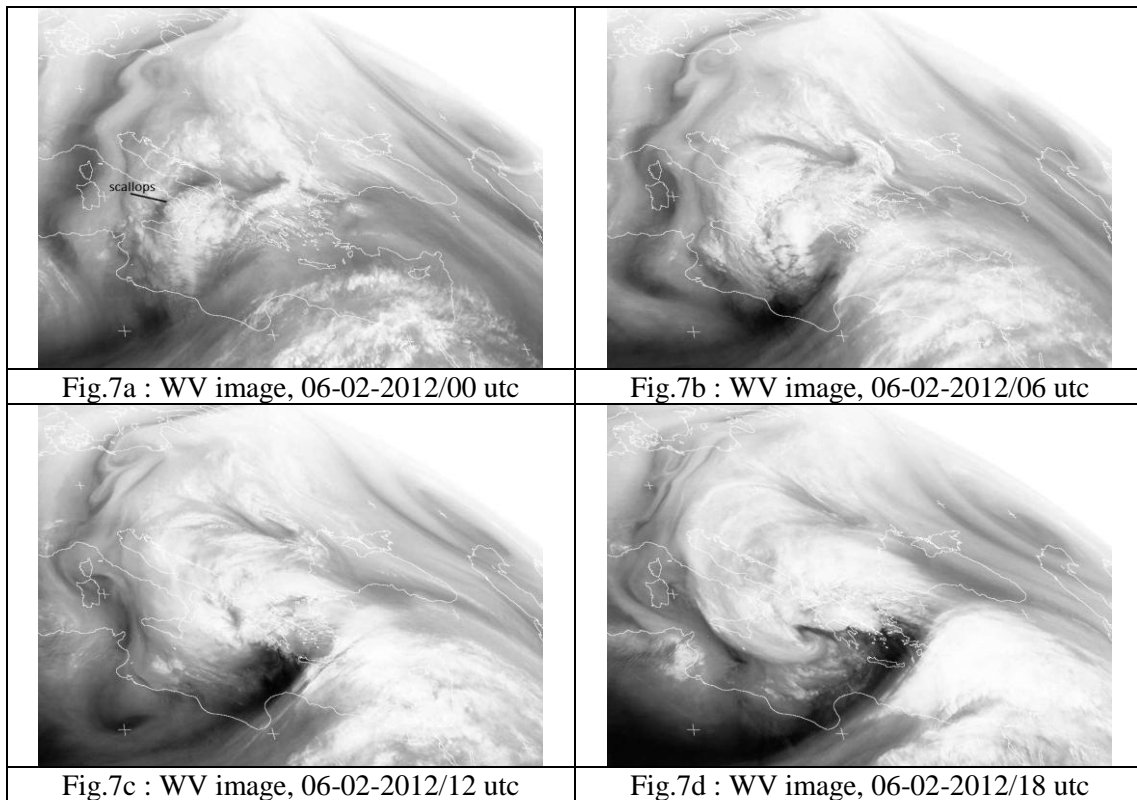


Fig.6: Mean sea level pressure contours by 2 hPa, 06-02-2012/18 utc

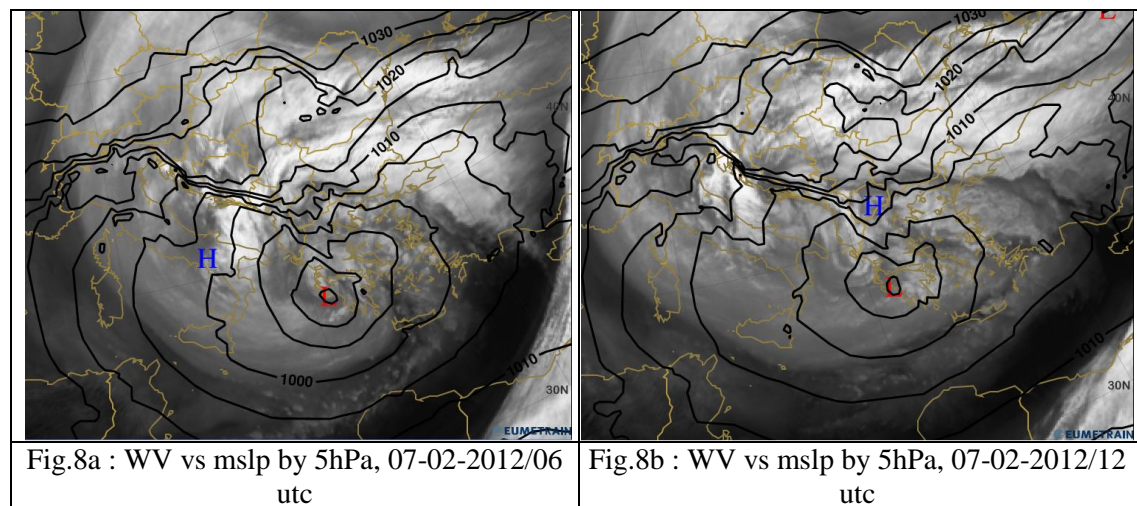
Looking at the satellite images from this event (fig.7a-d) several features of the conceptual models of synoptic and satellite meteorology can be identified. The position of the jet streams, a deformation area at the early stages of the developing cyclone (fig.7a), a baroclinic leaf on the cold side of the southern subtropical jet (fig.7a), some scallops at the northern side of the baroclinic leaf and consecutively, its evolution into a comma cloud and finally a vortex with a bend back structure of the occlusion. The relatively large dark spot at the coast of Lybia moving northward (fig.7b, 7c) shows a relative maximum in IPV (isentropic potential vorticity) (fig.4) that forms a tongue of stratospheric air extruding downward at lower levels. This is verified by the height of the 1.5 PVU surface (below 600hPa, fig.4). The dark dry slot in fig.7d is well aligned along the 300hPa flow.

* Images 7a-7d on the following page from www.dundee.ac.uk, using Meteosat's SEVIRI instrument at channel 5 (mid IR to WV, 5.35 – 7.15 μm)

** Images 7a-7d not corrected for earth's curvature



The rigorous circulation of the surface depression helps maintain strong winds over Greece on the following day (7th February) as well, retaining at the same time a prominent vortex with an occlusion form at WV6.2 images (fig.8a, 8b). By 07-02-2012/12 utc the rapid cyclogenesis is over, the surface low pressure system at the SE Ionian Sea starts to fill up with gradually relaxing winds and eventually splits up into smaller-scale vortices while making landfall.



All the above are summarized in the following quite fascinating Airmass RGB images from the archive of EUMeTrain. A mature cyclone with an occlusion is identified in fig.9a, and the reddish coloured stripe that surrounds almost the entire vortex is an indication of stratospheric air protruding downward into the troposphere. It coincides with the long black stripe in the WV image (fig.7d) (and therefore dry stratospheric air). The warm front band shown by the high clouds in white on the right side marks the boundary of air masses of different temperature. 18 hours later as depicted in fig.9b, the warm front band is displaced further to the east and a deep cyclonic vortex is situated over eastern Mediterranean. Within the occlusion a comma cloud and an enhanced cumulus area behind the frontal cloud band can be identified.

Airmass RGB images from Eumetrain

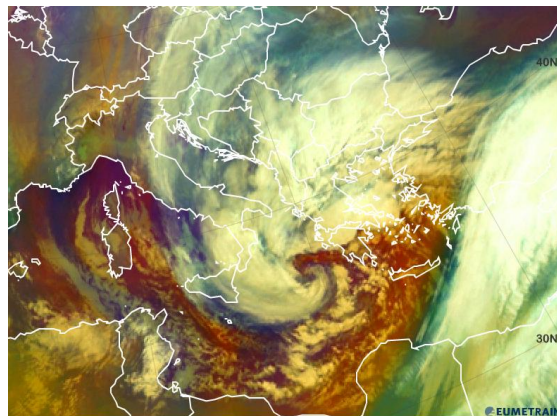


Fig.9a : 06-02-2012 at 18 utc

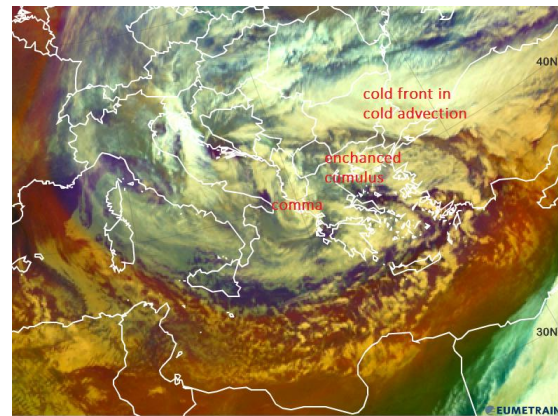
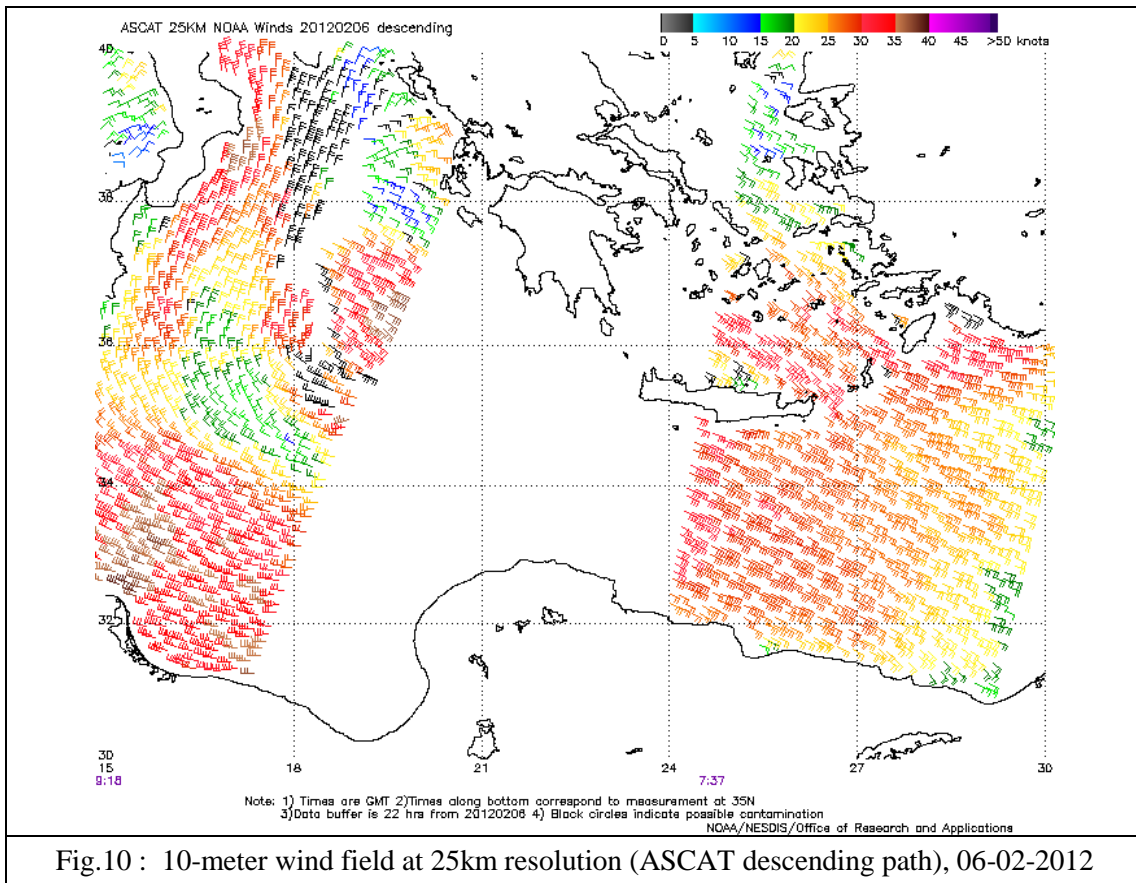


Fig.9b : 07-02-2012 at 12 utc

Assessment of the marine environment

An overall insight into the wind circulation close to the sea surface in the case of the rapid cyclogenesis described above is given through satellite retrieved scatterometry data from ASCAT, a C band instrument aboard the EUMETSAT METOP satellite. The ASCAT ocean surface winds are a 10-meter neutral stability wind. ASCAT did not always provide a full view of the depression's wind patterns due to its coverage limitations, but the depiction of the wind fields on the available images shows additional information on the position of the surface fronts and the location of pressure minima.

The 10-meter wind field as measured by ASCAT with a 25km resolution is depicted on the following image and corresponds to time measurement between 7 and 9 utc at 35N on February 6, 2012. A wide area of wind speeds exceeding 30kts covers the south part of eastern Mediterranean and the position of the low pressure system along with the frontal/convergence wind patterns are quite prominent.



The same wind field at 50 km resolution and the ambiguity product are shown below (fig.11a, 11b). The wind vector retrievals coloured in black, which are flagged as potentially being corrupt according to the KNMI quality flag, correspond to the directional ambiguity in areas of convergence. The ASCAT winds discontinuity enables the location of the surface frontal position. The UK Met Office analysis (fig.12 a-c) confirms the presence of a surface front and its position coincides quite well with the area of directional ambiguity in the wind field.

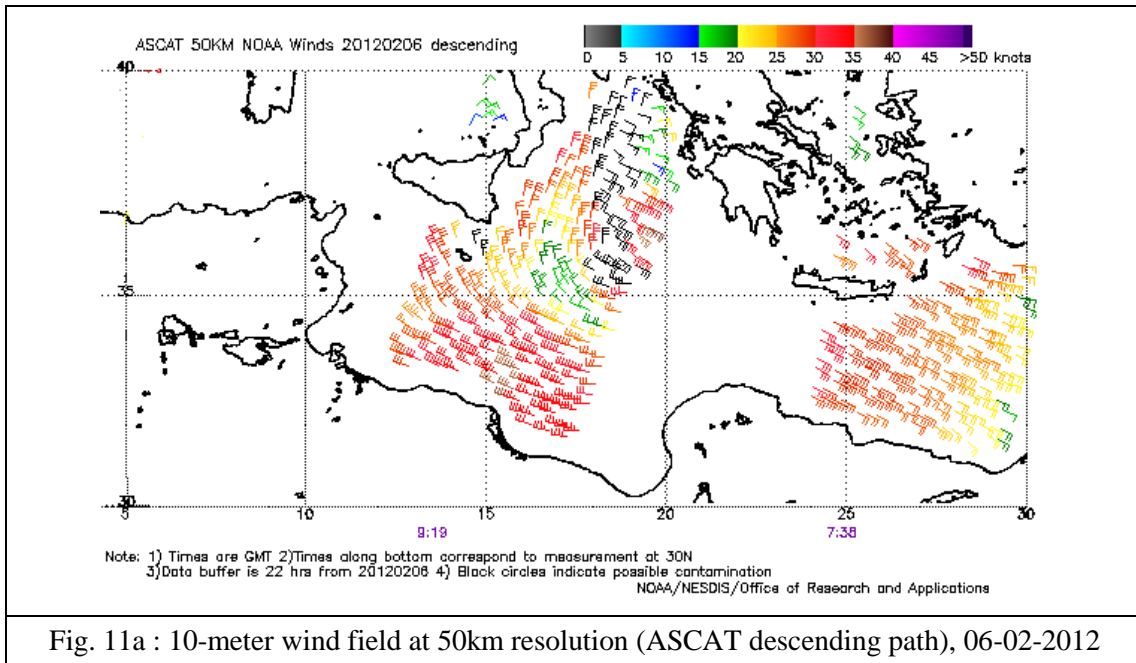


Fig. 11a : 10-meter wind field at 50km resolution (ASCAT descending path), 06-02-2012

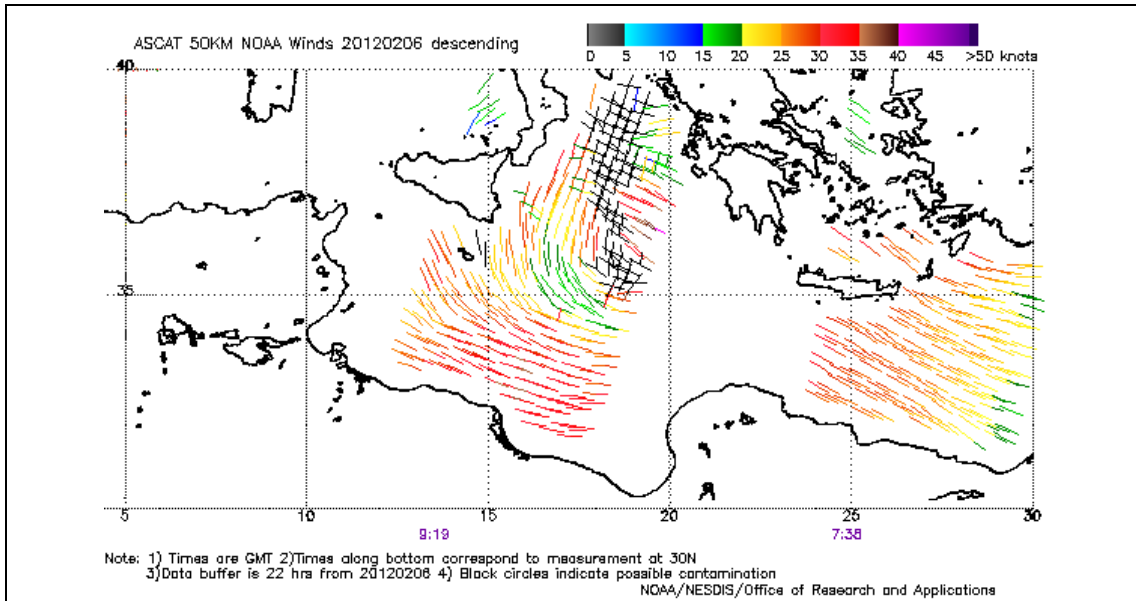
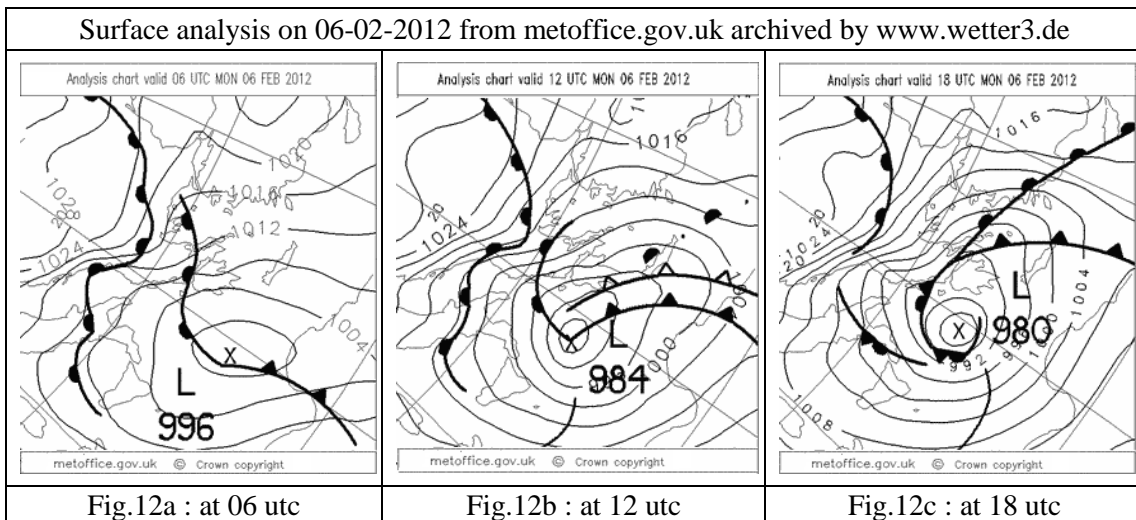
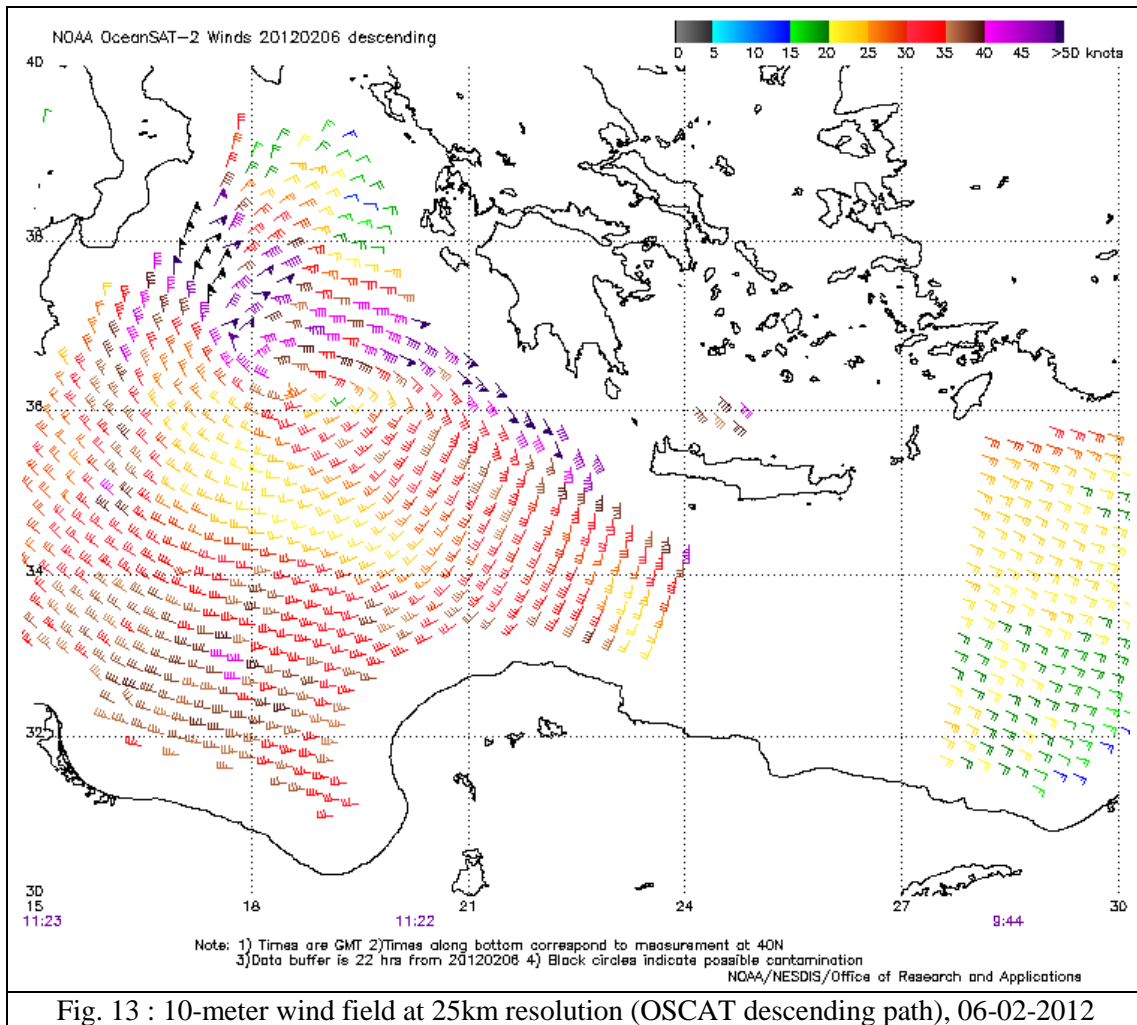


Fig. 11b : Directional ambiguity of 10-meter wind field at 50km resolution (ASCAT descending path), 06-02-2012



The pressure begins to fall significantly after 06-02-2012/06 utc, as by now the surface depression is right below the left exit area of a jet streak (70-80 kts at 300 hPa, yellow contours in fig.4) and stratospheric air is reaching its lower level (~700hPa, purple contours in fig.4), resulting in speeds exceeding 40kts in the surface wind field, as illustrated in the following ocean surface wind vector retrievals from OSCAT at 25km resolution (fig.13) and correspond to time measurement between 9 and 11 utc at 40N.



The OSCAT is a Ku-band conically scanning scatterometer system aboard the Oceansat-2 satellite and its ocean surface wind retrievals also represent a 10 meter neutral stability wind. The flagged as potentially being contaminated by rain wind vector retrievals are coloured in black and such flags appear on the upper left side of the vortex, within which as expected, precipitation is occurring. The current rain flag is under-flagging for rain (from manati.star.nesdis.noaa.gov website), so data from these areas is less trustworthy.

A few hours later in the WindSAT retrievals shown on the next image (fig.14) which correspond to time measurement at 16 utc at 30N, the overall wind field is enhanced with speeds exceeding 45kts. The position of the low-pressure system with the circulation around it are evident and the northerly winds marked by the black arrow represent an 180° ambiguity, since are inconsistent with the southerly flow below.

The WindSAT wind retrievals from the first space-borne polarimetric microwave radiometer are at a 10m height assuming neutral stability as well, and are derived from WindSAT microwave brightness temperatures measurements with a retrieval scheme that is purposely developed to explore wind retrieval performance in the storm environment (from manati.star.nesdis.noaa.gov website). The current "rainflag" does not flag all contaminated retrievals. Yet a wide area of black barbs affected by the precipitating clouds (fig.17b) around the rigorous surface depression can be identified.

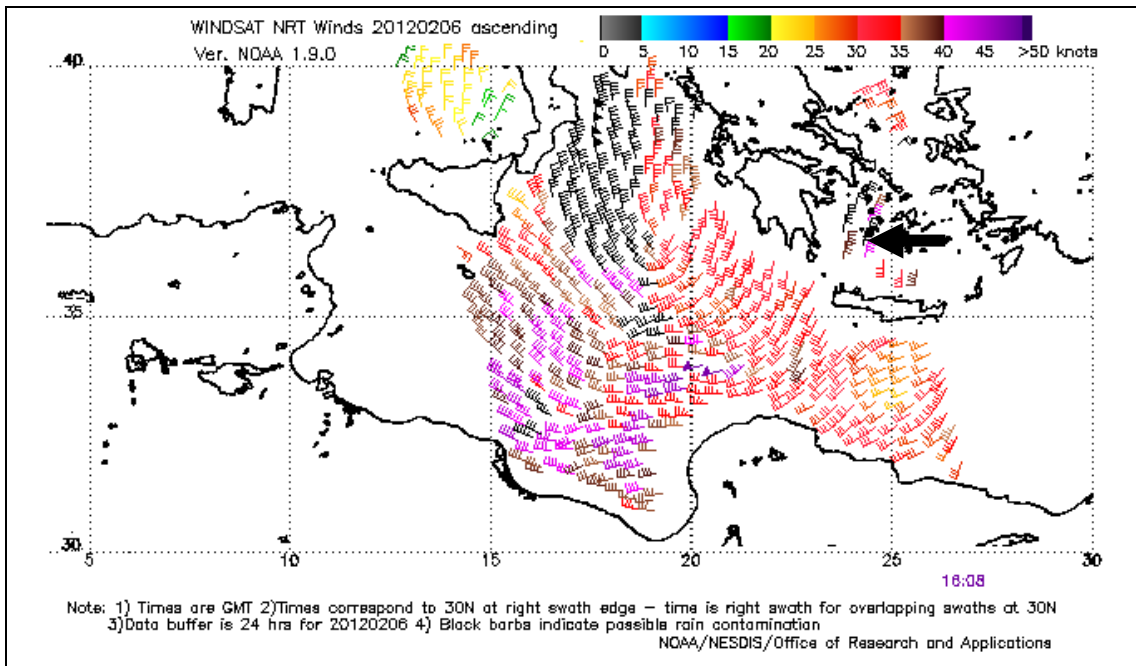


Fig. 14 : 10-meter wind field at 25km resolution (WindSAT ascending path), 06-02-2012

The next image (fig.15) shows the last available satellite passage from that day again from ASCAT, corresponding to time measurement between 18 and 20 utc at 35N. Although a large portion of the maritime area of interest lays just below the satellite's swath gap, 45kts wind speeds expanding from 15E to 27E are retrieved. The time coincides with the observed minimum pressure of 982 hPa at 18 utc.

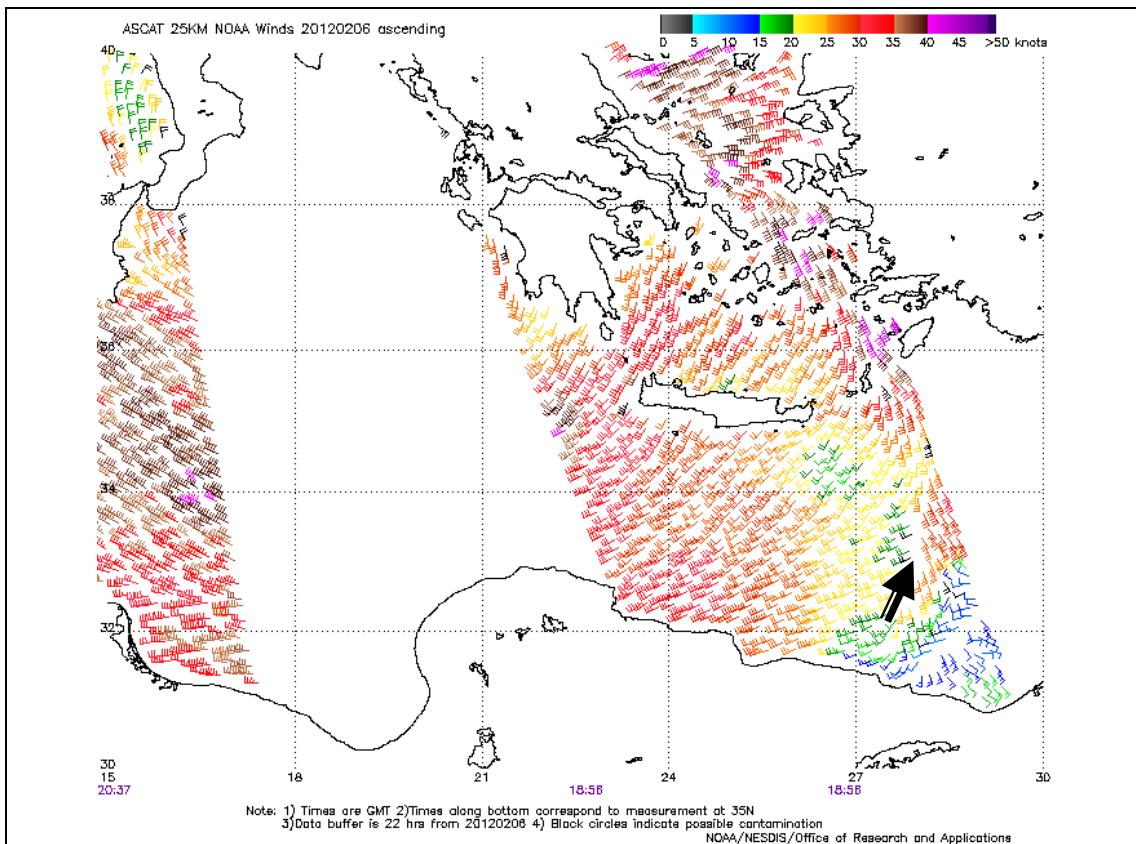
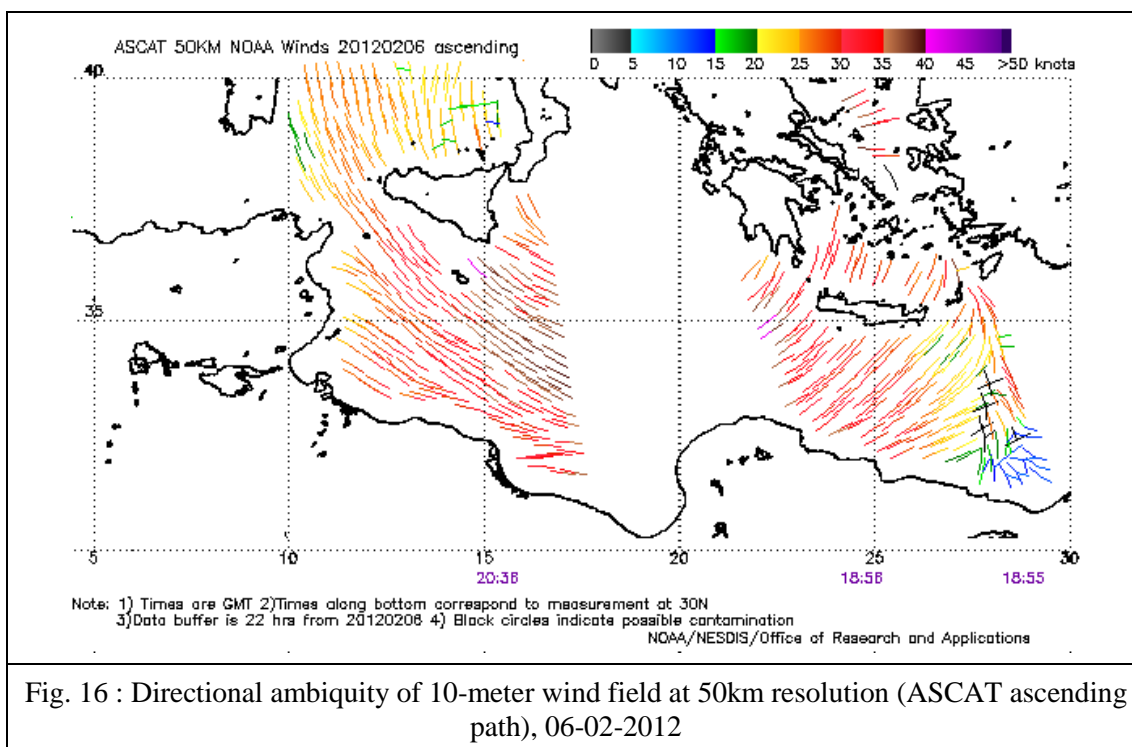


Fig. 15 : 10-meter wind field at 25km resolution (ASCAT ascending path), 06-02-2012

To the east of the previous image (fig.15) a wind convergence line (marked by the black arrow) is found in the ASCAT wind product. It connects with the position of the surface front at 18 utc as depicted in fig.12c. Again the ambiguity product of the same wind field in 50km resolution cited below (fig.16) depicts this area of uncertainty at the bottom right side.



A comparison of ASCAT winds with ECMWF NWP products is given next. The ASCAT wind field on fig.17a – 17d corresponds to time measurement 9.19 utc at 30N from the 50km resolution retrievals and the overlaid NWP products at 12 utc analysis from ECMWF. The small displacement in the low pressure system’s centre between the ASCAT field and the 10m wind field in fig.17c is probably due to this difference in time. The ECMWF 10m wind speeds range between 25 to 40kts around the system’s centre (fig.17c). The north-westerly wind barbs next to the opposing flow marked by the green arrow in fig.17a support the idea that the ambiguity removal scheme on ASCAT wind processing did not make the right choice (180° ambiguity).

In fig.17b, 17d a combination of the ASCAT wind data with satellite images is plotted. The south-easterly flow on the right of fig.17b coincides with the warm advection area and the sharp southeast-northwest temperature gradient between the warm and moist tropical air mass and the colder and drier one, as previously described. The position of the centre of the depression is just below the prominent cloud head in the IR10.8 image. The Severe Storm RGB product in fig.17d depicts the position of convective precipitation (yellow arrow) in accordance with the rain contamination flagged wind barbs mentioned above.

ACSAT winds with ECMWF NWP and satellite products on 06-02-2012/12 utc from eumetrain.org

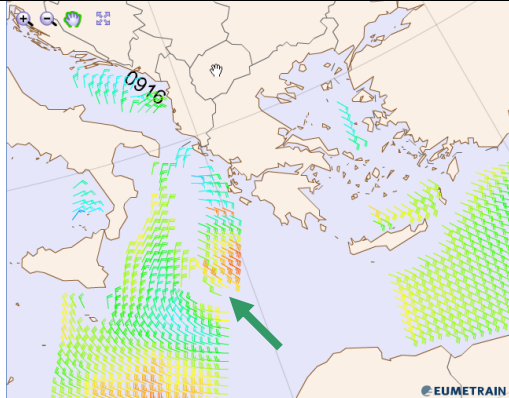


Fig.17a : ASCAT winds

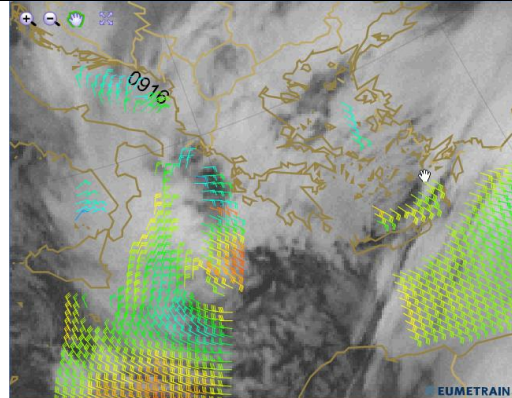


Fig.17b : ASCAT winds vs IR10.8 image

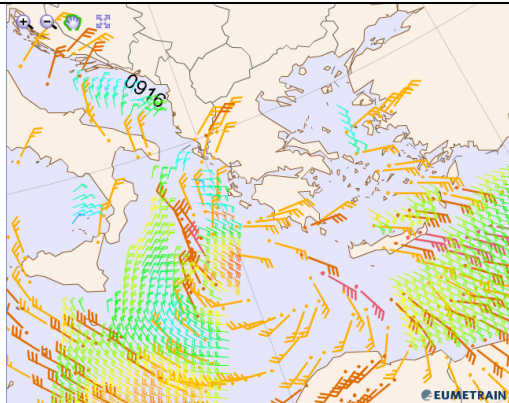


Fig.17c : ASCAT winds vs 10m windspeed

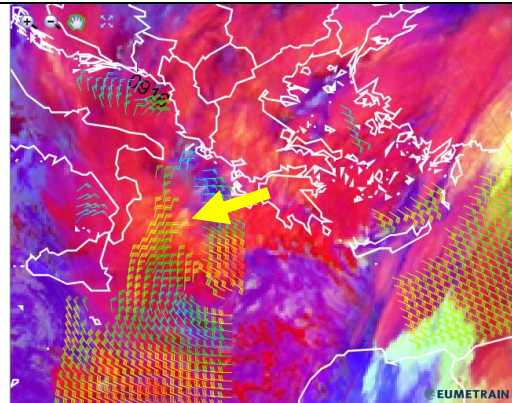


Fig.17d : ASCAT winds vs SevereStormRGB

The low-pressure surface system develops in a region where the sea surface temperature (SST) ranges from around 23 °C south of 35°N to between 14 and 18 °C north of 35°N (fig.18a, 18b). It continues its northerly path remaining over the small SST gradient area until the middle of the following day, 7th February before making landfall.

Sea Surface Temperature measurements from WindSAT

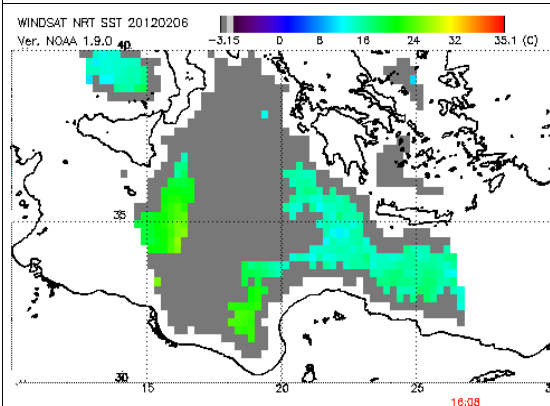


Fig.18a : 06-02-2012

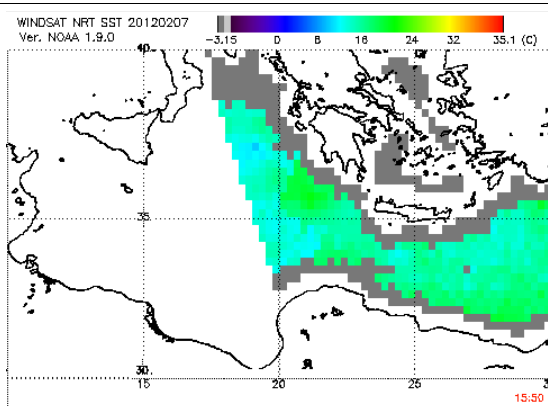
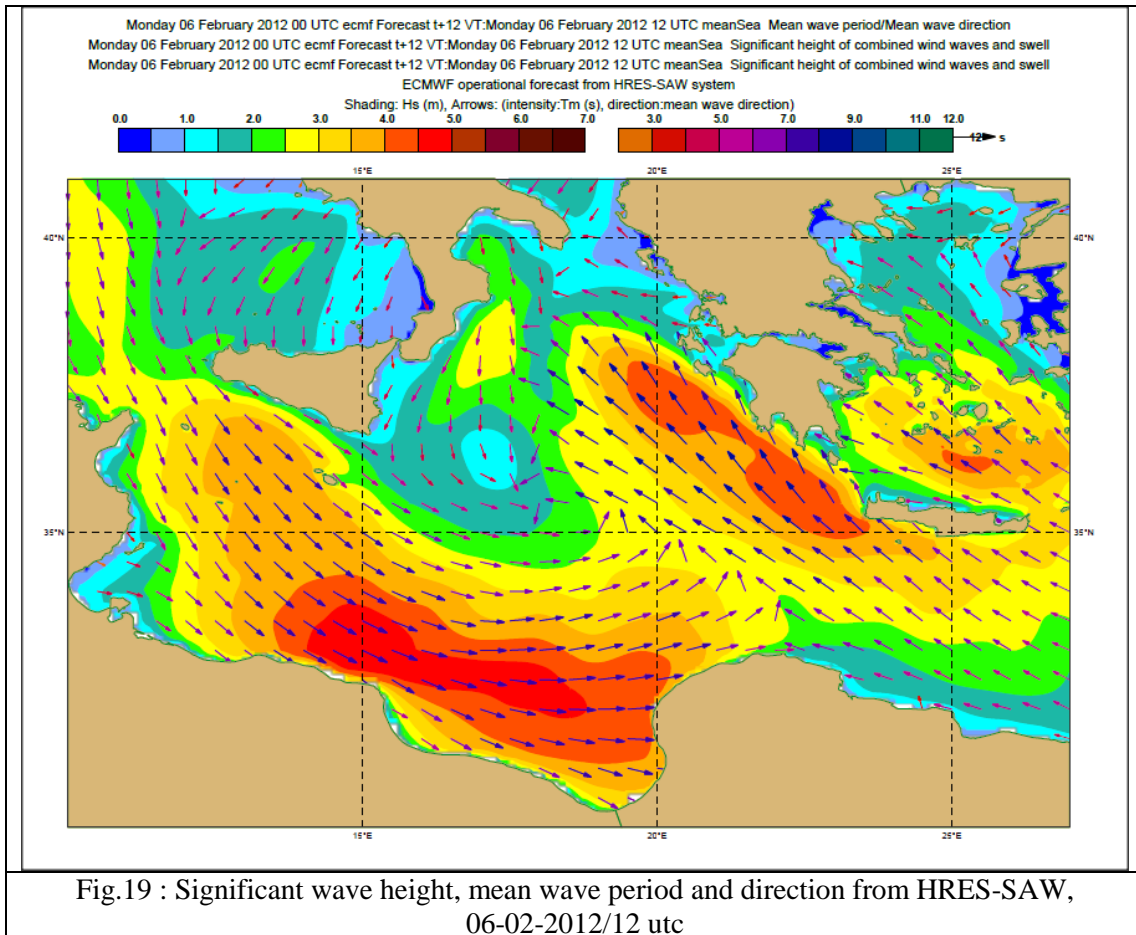


Fig.18b : 07-02-2012

Powerful seas and high waves derive from the forceful forcing of these strong winds to the sea surface. The HRES-SAW version of the ECWAM model forced by the forecasted wind field from the ECMWF atmospheric model presents this situation, with forecasted significant wave height of combined wind waves and swell up to 7m, from 06-02-2012/18 utc to 07-02-2012/06 utc, period during which sustained surface winds of 40 kts exist. Later on the sea begins to abate (fig.25).

This is illustrated in the following figures (fig.19 – fig.25) of significant wave height, mean wave period and direction, courtesy of Jean Bidlot from ECMWF. The ASCAT wind field on 06-02-2012 at around 18 utc (fig. 20) and on 07-02-2012 at around 9 utc (fig.24) are cited in between, for a direct correlation between surface winds and wave height.



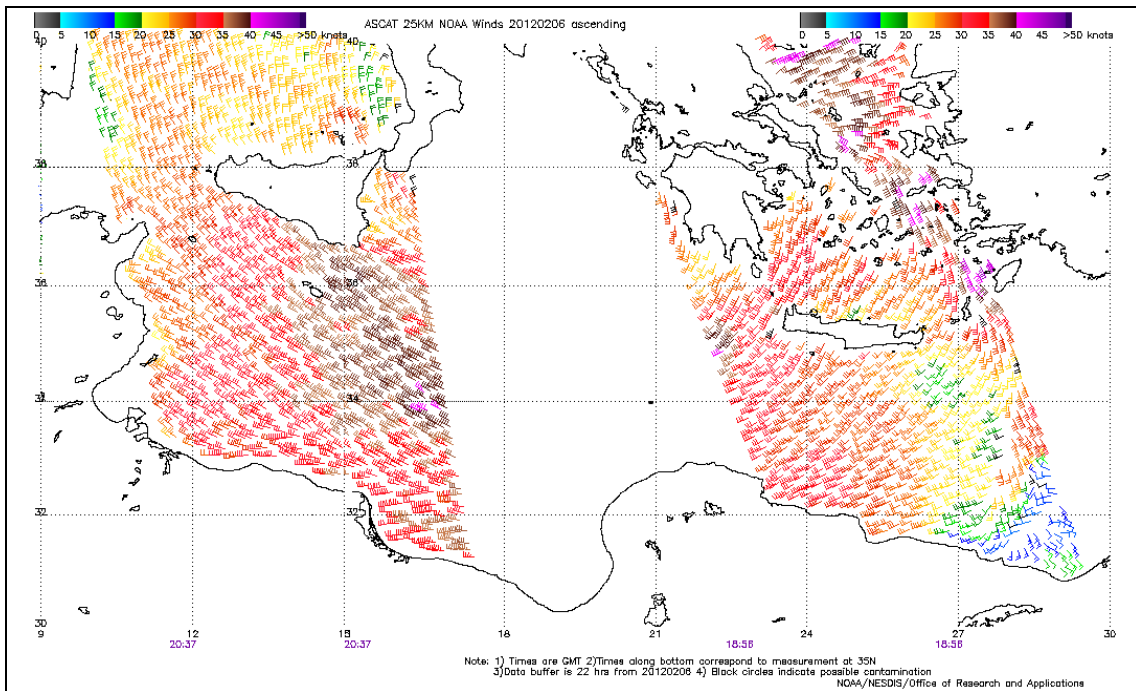


Fig.20 : 10-meter wind field at 25km resolution (ASCAT ascending path), 06-02-2012/18 utc

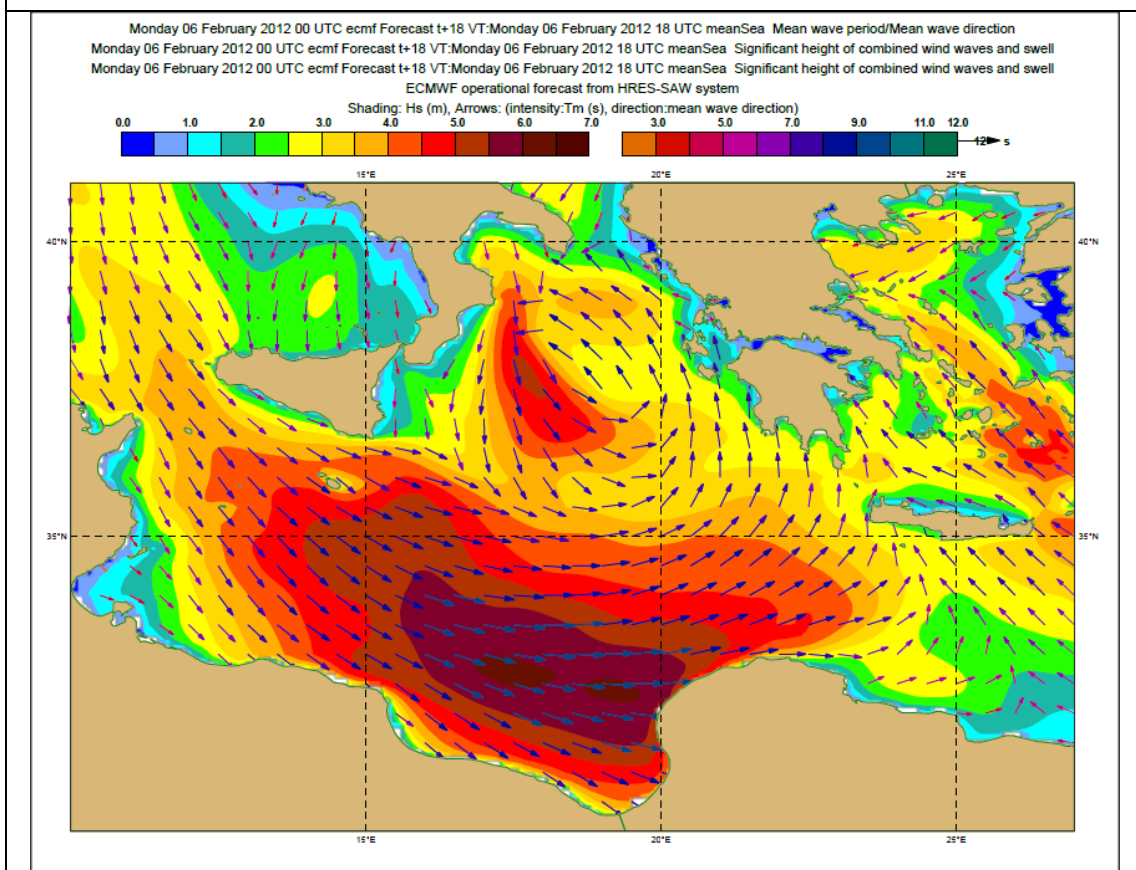


Fig.21 : Significant wave height, mean wave period and direction from HRES-SAW, 06-02-2012/18 utc

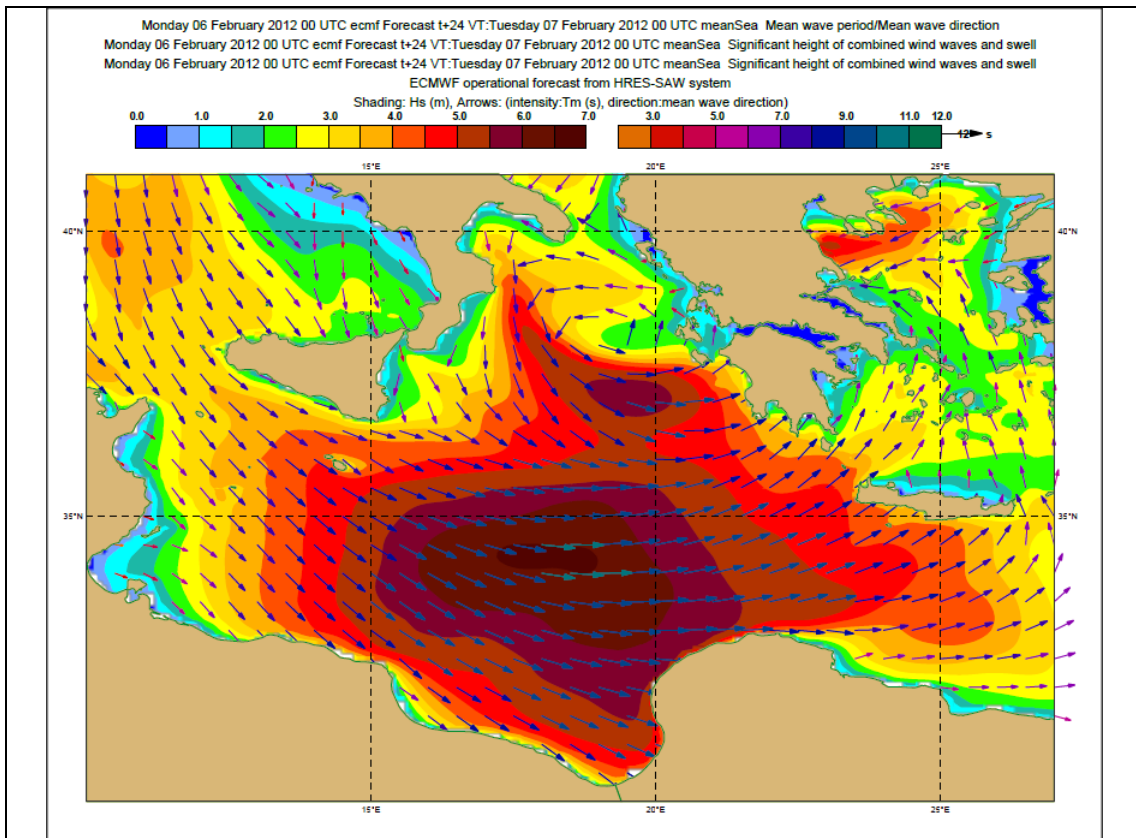


Fig.22 : Significant wave height, mean wave period and direction from HRES-SAW, 07-02-2012/00 utc

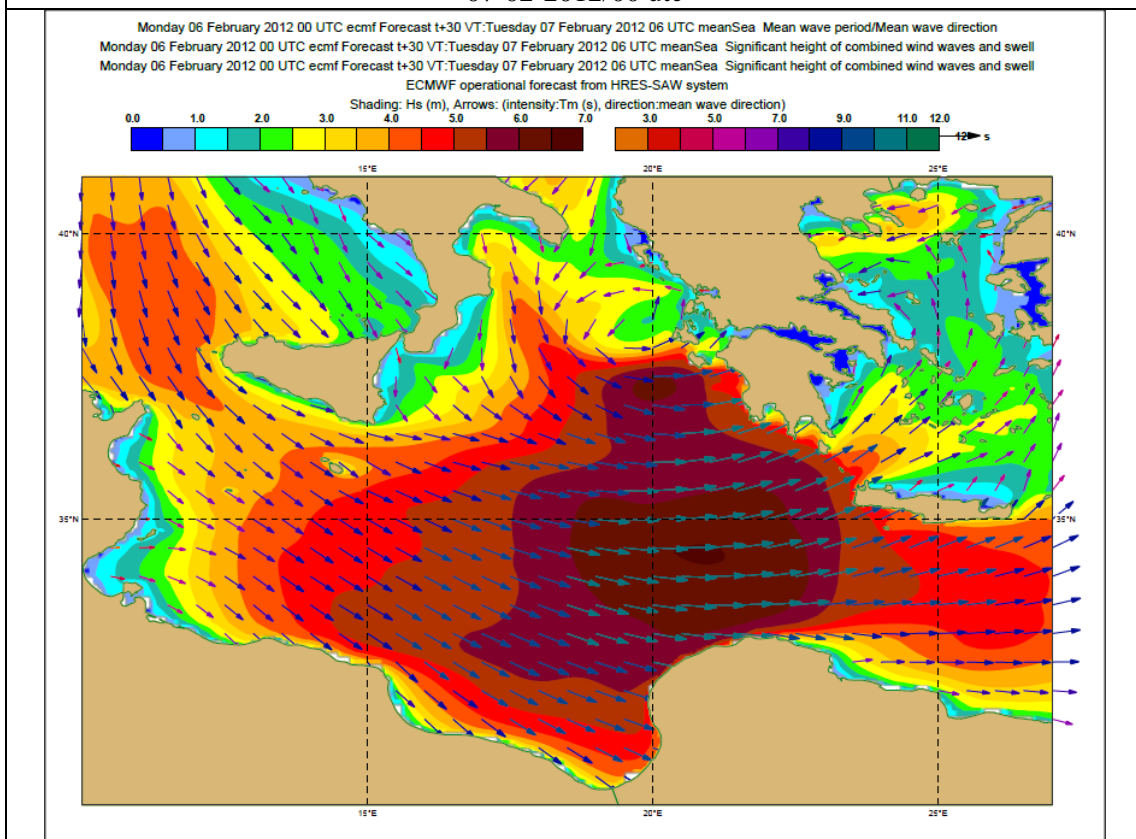


Fig.23 : Significant wave height, mean wave period and direction from HRES-SAW, 07-02-2012/06 utc

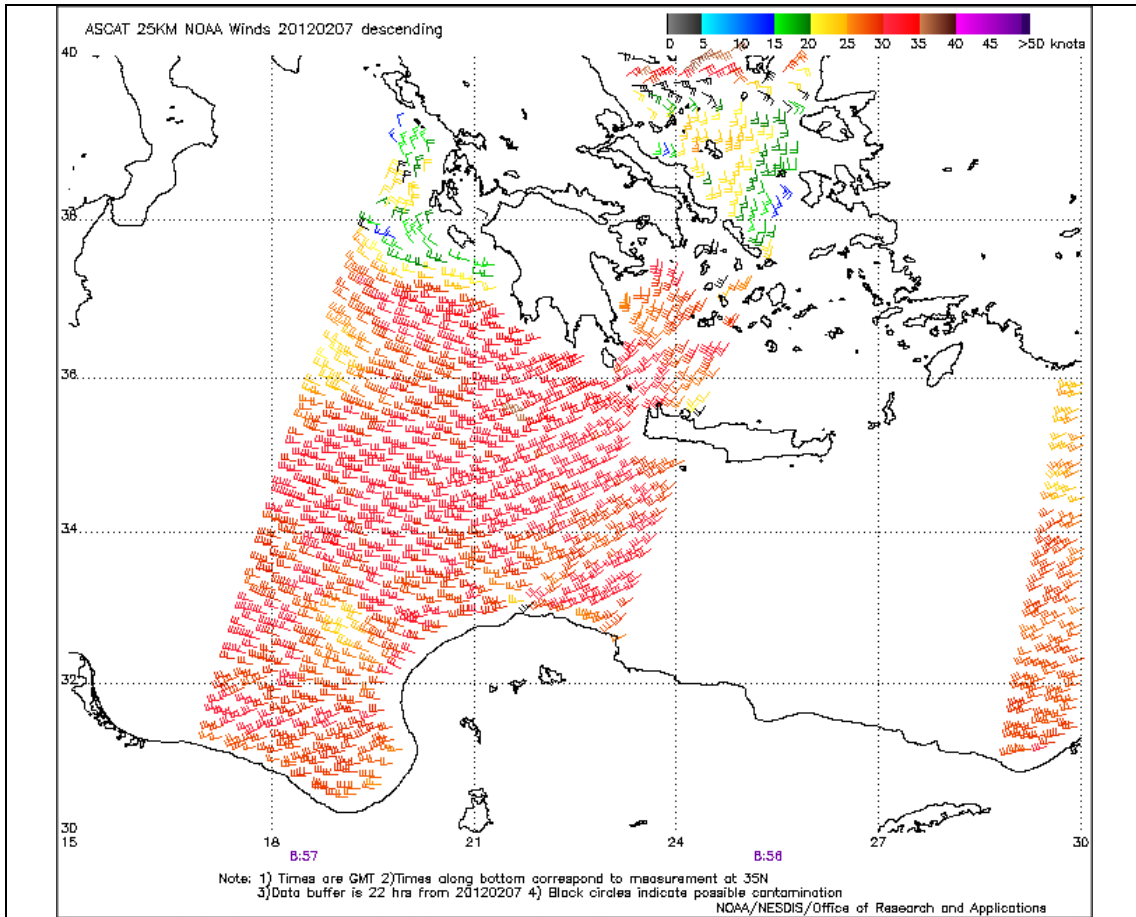


Fig.24 : 10-meter wind field at 25km resolution (ASCAT descending path),07-02-2012/09 utc

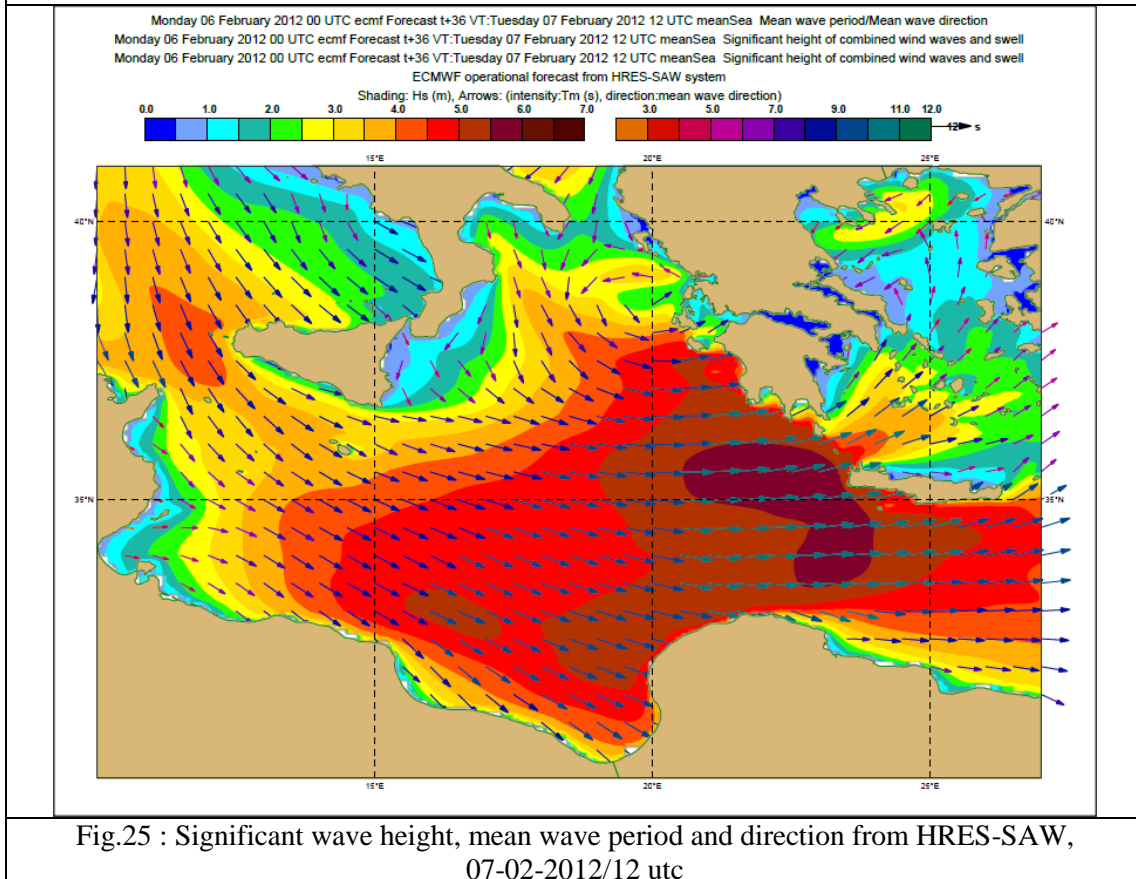


Fig.25 : Significant wave height, mean wave period and direction from HRES-SAW, 07-02-2012/12 utc

Conclusions

The surface depression presented in this case showed strong convective activity that was quite well depicted by satellite imagery. An impressive dry stratospheric intrusion and the jet stream played decisive role on its dynamics, development and strength, bringing a strong flow of warm air over east Mediterranean that was rapidly displaced by cold air masses. The organized convection and strong wind field were the result of a rapidly evolving cyclone lasting between 6th and 7th February, 2012.

Mean wind speeds of 41 kts and gusts reaching 60 kts were recorded as well as large amounts of precipitation, affected not only coastal but continental areas too. It caused 2 casualties, which resulted from drowning, significant damage and destruction, with trees being uprooted, extensive flooding, electrical grids being affected, cutting off power to some islands and serious trouble in marine communications and transportation in general.

The need of reliable forecasting has a direct correlation with the hazards and effects of such phenomena, especially for the high vulnerable marine and coastal environment. Satellite and altimetry imagery and data therefore play an essential role in both forecasting and modelling.

* All satellite wind data from <http://manati.star.nesdis.noaa.gov>